Operational Use of Near-Real-Time Sea Surface Directional Wave Spectra Generated from NOAA Scanning Radar Altimeter Range Measurements

Edward J. Walsh, Principal Investigator, retired
Code 614.6, NASA Goddard Space Flight Center, Greenbelt, MD 20771
office 303-497-6357
cell 303-579-7811
edward.walsh@noaa.gov

November 30, 2009 - Final Report

1. INTRODUCTION

The NOAA Wide Swath Radar Altimeter (WSRA) is functioning well and its future looks very promising. There is a $300K cap on the funding available from the NOAA Small Business Innovation Research (SBIR) program, yet under that program ProSensing was able to build the WSRA state of the art replacement for the NASA Scanning Radar Altimeter (SRA) which fifteen years earlier had cost $1,000K in addition to several man-years of civil service engineering time. ProSensing did a remarkable job and the WSRA made several flights into hurricanes aboard one of the WP-3D aircraft of the NOAA Aircraft Operations Center (AOC) during the 2008 season.

Based on the initial buoy comparison with the directional wave spectra derived from the WSRA hurricane data, the Joint Hurricane Testbed (JHT) decided in mid-March 2009 to fund a 2-year ProSensing proposal to bring the WSRA to full operational status and unattended operation. But due to internal delays within NOAA, ProSensing was not put under contract until September 29, 2009, and ProSensing was not able to prepare for the 2009 hurricane season. As a result, unattended operation has not yet been implemented on the WSRA and an operator's manual relating to it could not be completed within this effort. That aspect will be worked on as part of the continuing ProSensing effort. This report will indicate the status of the WSRA and its signal processing, describe the insights gained into this innovative system, and project its schedule for operational status.

2. WSRA WAVE TOPOGRAPHY MEASUREMENTS

ProSensing was able to fabricate an improved system on less that a third of its predecessor's budget by developing a design that was two orders of magnitude more complex. The NASA SRA measured the time of flight of a short pulse (6 ns, 0.9 m range extent) whose 1.5 KW peak power was achieved with a Klystron that cost $300 K by itself. The NOAA WSRA as designed and built by ProSensing transmits a long, chirped pulse with a peak power of only 20 W which achieves comparable sensitivity and range resolution as the old system without using a costly high power EIK based transmitter. The SRA used a dielectric lens to form a narrow beam which was scanned mechanically. As the SRA hardware aged, the beam angles began deviating from their nominal values, degrading the data. The WSRA uses digital beam forming with no moving parts which is much more stable.

Figures 1 and 2 below are repeated from the mid-year report on the present effort (Fig. 3 and 4 in that report). They demonstrated that the WSRA produced good quality wave topography and that the wave characteristics extracted from the directional wave spectrum generated from the topography agreed very well with Buoy 42001 in the Gulf of Mexico. Even though the results were excellent, I indicated in the mid-year report that there appeared to be a hardware problem causing errors in the raw data that needed to be identified and corrected. This report examines that concern in detail.

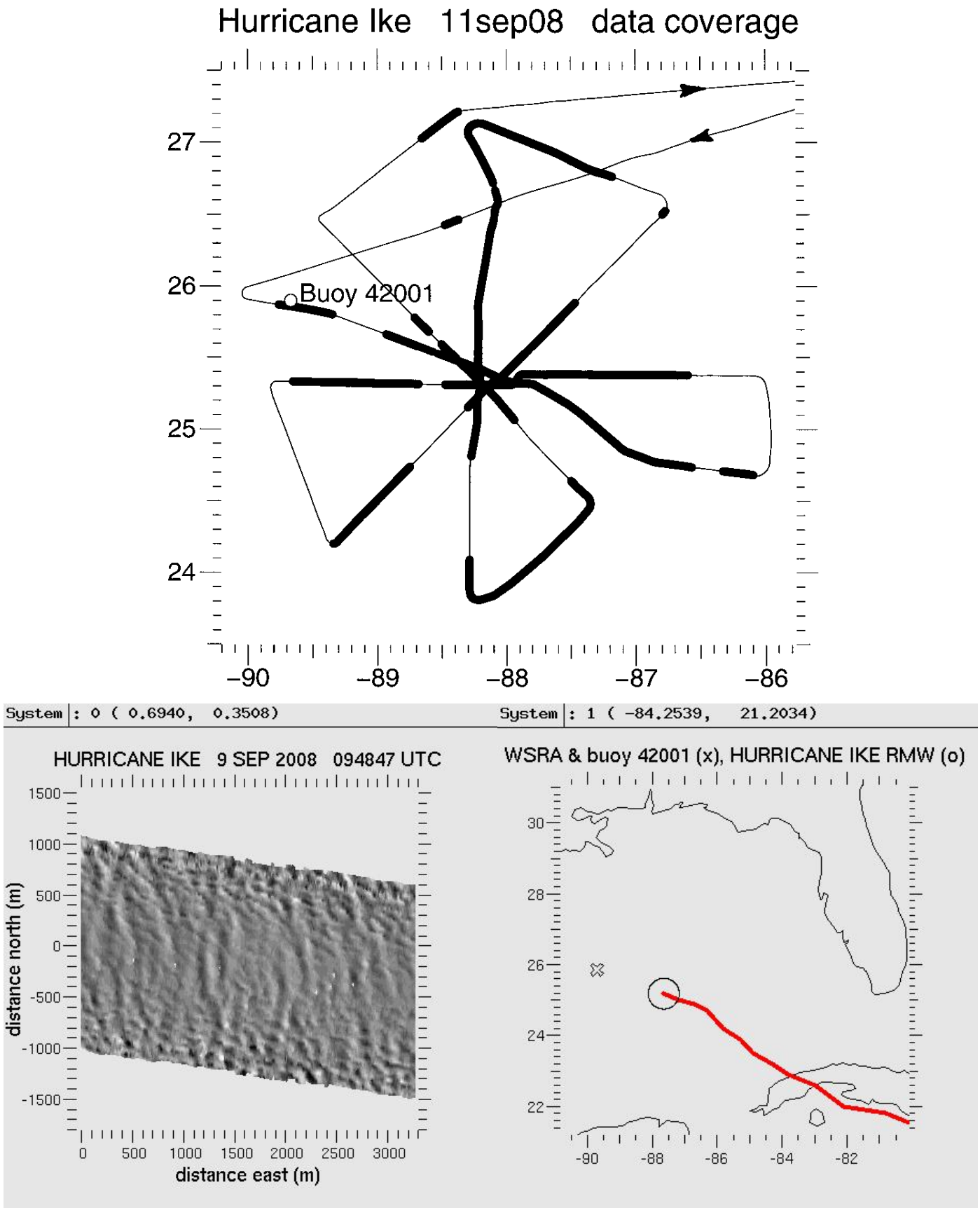

Figure 1. WSRA data coverage in the vicinity of Hurricane Ike (thick segments, top panel). WSRA gray-scale coded wave topography at Buoy 42001 (bottom left panel, mislabeled as 9 instead of 11 SEP). Bottom right panel indicates Hurricane Ike track (red) and its RMW (circle) with the location of the WSRA and Buoy 42001 indicated (X).

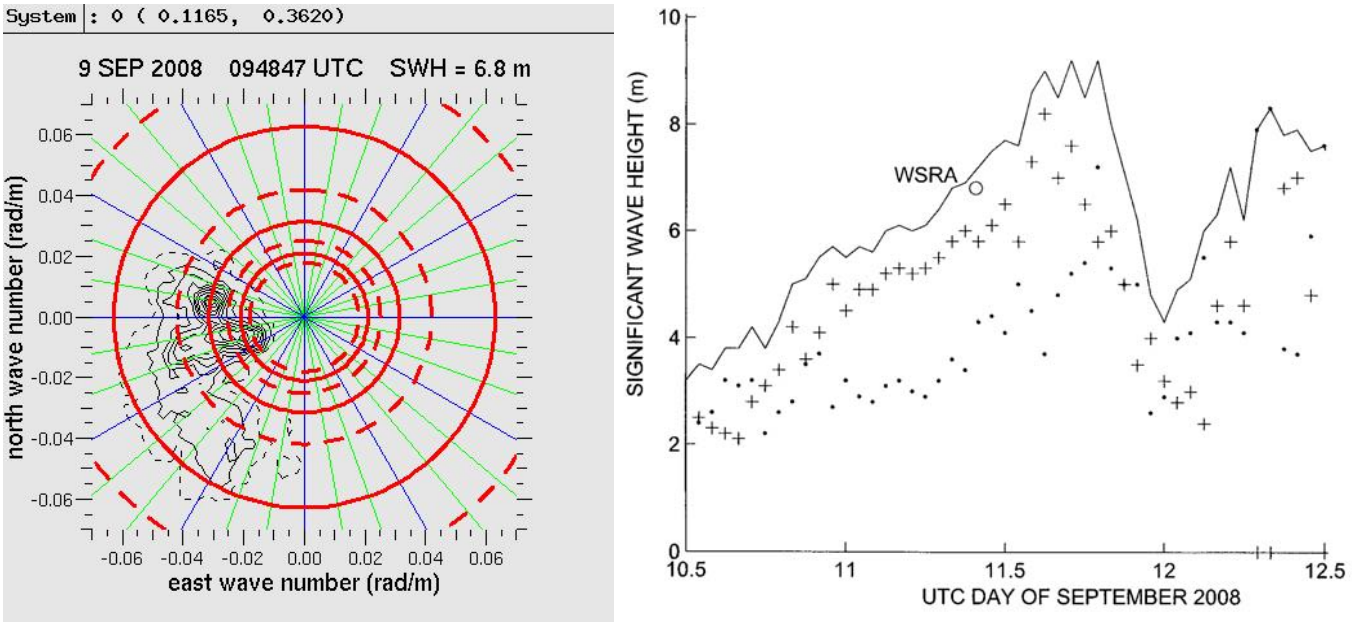

Figure 2. Left panel - directional wave spectrum generated from the wave topography in Figure 1. The nine solid contours are at equal intervals from 0.9 to 0.1 of the peak spectral density. The dashed contour is at the 5% level. The three solid red circles indicate wavelengths of 100, 200 and 300 m (outer to inner) and the four dashed circles indicate wavelengths of 75, 150, 250 and 350 m. Right panel - Buoy 42001 wave height variation, total(-), swell(+), sea(.), and the WSRA (o) value.

Figure 3 shows the WSRA range measurement geometry in proportion. Waveforms of return power versus range are generated within a range window (dashed curves) whose near limit is generally set about 100 above the range to mean sea level (MSL) at nadir and whose far limit is great enough to encompass the largest range to the sea surface at the edge of the swath.

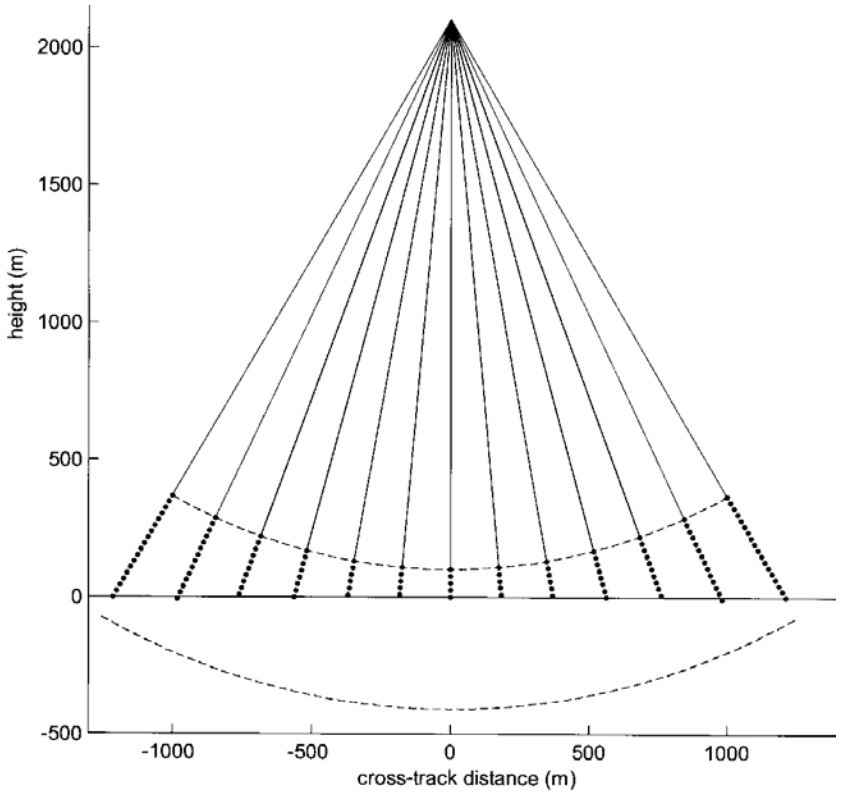

Figure 3. Nominal range measurement geometry for the WSRA.

The WSRA range determination is much more complicated than the SRA measuring the time of flight of a short pulse. To achieve a usable signal level with only 20 watts of peak power the WSRA transmits a very long chirped signal (2900 m range extent at 3000 m altitude). It then mixes the returning signal with another chirped signal offset in time so the result will be a constant intermediate frequency (IF) if the range is equal to the nominal range. A signal returning from a range different than the nominal range will result in a frequency offset from the IF with the amount of the offset being proportional to the difference in range.

Figure 3 corresponds to an aircraft height of 2100 m and the 13 radials extending from the antenna to the near edge of the range window represent 13 of the 80 narrow beams that the WSRA produces to interrogate the sea surface. The dots extending from the near edge of the range window to the sea surface represent range increments within the return waveform. For clarity they are spaced at 25 m increments instead of the nominal value of 1.0836 m. The last dot would contain the power backscattered from the sea surface. Greater ranges (not shown) would contain only noise power. The most simple determination of the range to the sea surface within each antenna beam would be to multiple the magnitude of the range increment by the number position within the waveform that had the maximum power, then add the range to the near edge of the window. The range determinations would fluctuate about MSL because of the presence of waves, but with a swath more than 2 km wide, a parabola fitted through the ranges would be a horizontal straight line.

When the WSRA range data from Hurricane Ike were process into wave topography, the mean sea surface was not horizontal but curled upward on both sides of nadir or curled downward. This is illustrated in Figure 4 and would occur if the actual range increment within the waveforms was different than the nominal value. The same 13 beams of Figure 3 are represented in Figure 4, but the dots indicating the nominal range increment within the window are spaced at 10 m intervals instead of 1.0836 m and the vertical dimension has been stretched by a factor of 3, distorting the angles.

The top panel of Figure 4 shows the same situation as Figure 3 where the actual range increment is equal to the nominal value. The middle panel shows that situation that would result if the actual range increment were 15% smaller than the nominal value. It would take more range increments to reach the sea surface because of their smaller value. When the ranges were computed using the nominal increment value it would push the total ranges beyond MSL everywhere, but more so near the edges of the swath where more range increments were involved, curving the mean surface downward.

The bottom panel of Figure 4 illustrates the situation if the actual range increment were 15% larger than the nominal value. It would then require fewer increments to reach MSL. When those fewer increments were weighted by the smaller nominal range quantization, it would pull the sea surface upward everywhere, but to a greater extent at the edges of the swath where more intervals were involved and the sea surface would curve upward.

I modified the post-processing software to automatically determine the value of the waveform range increment that would produce a flat mean sea surface for each set of 80 cross-track elevations. That result for 900 consecutive raster lines (3 sets of 300 raster lines) is shown in Figure 5. The horizontal line is the nominal range increment value of 1.0836 m. Figure 5 seems to suggest that there was an unstable problem of undetermined origin in the range determining hardware. But after the actual cause of the problem was recognized, it was realized that the range hardware did not have a problem.

The probability of a range increment problem seemed high initially because it did not seem reasonable that the antenna beam angles could have been varying with time. But, as with the range measurements, the WSRA antenna system is an order of magnitude more complex than that of the SRA. The SRA operated at 36 GHz and the left panel of Figure 6 shows the dielectric lens it used to form a narrow beam (1° 2-way). The SRA beam was scanned mechanically by an internal rotating mirror. The WSRA antenna (right panel) operates at 16 GHz and sequentially transmits its chirped pulse on each of 62 along-track linear strip

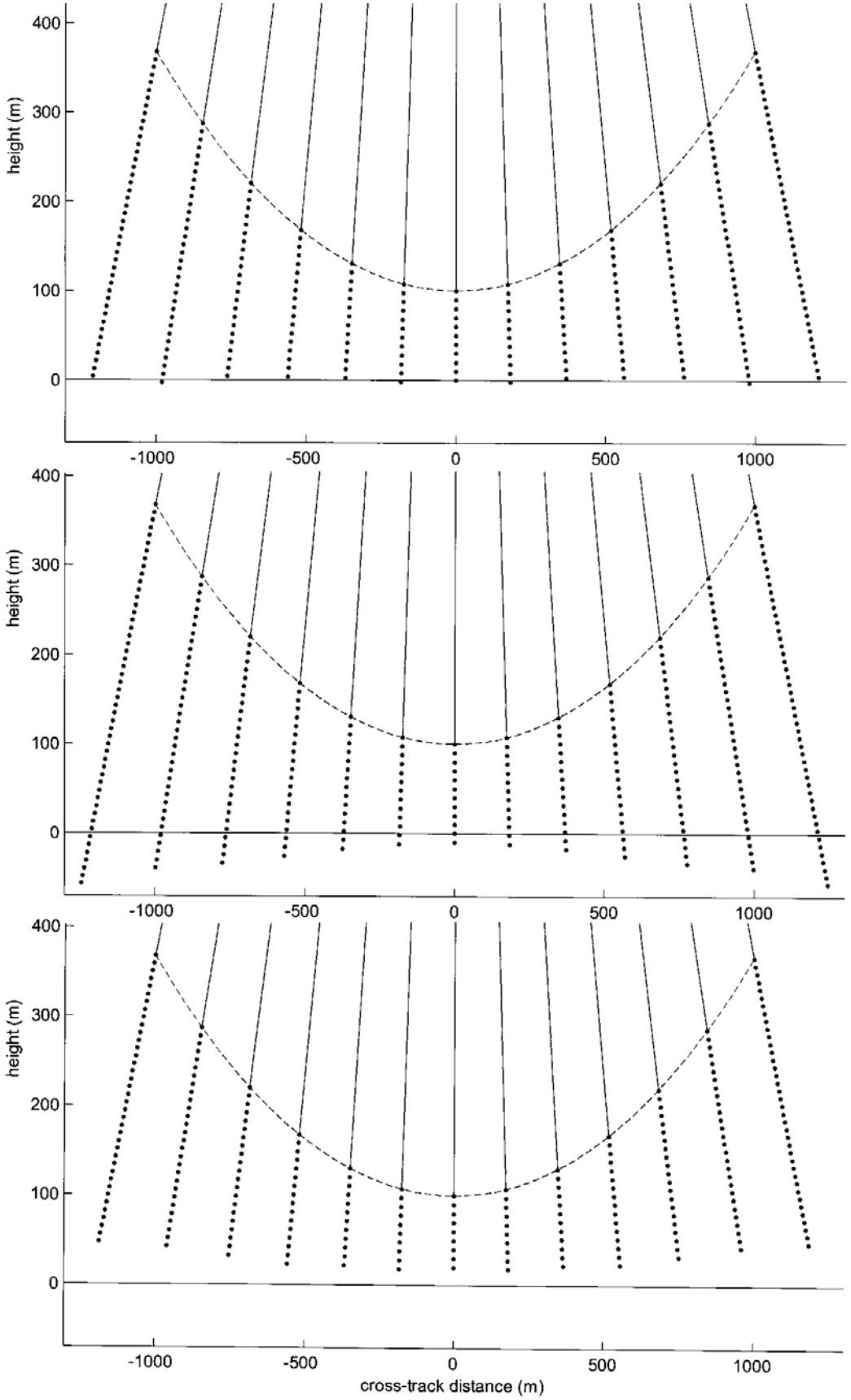

Figure 4. Effect on the apparent range to the sea surface if the nominal and actual range increments within the window are equal (top), the actual range increment is 15% smaller than the nominal value (middle), or the actual range increment is 15% larger than the nominal value (bottom).

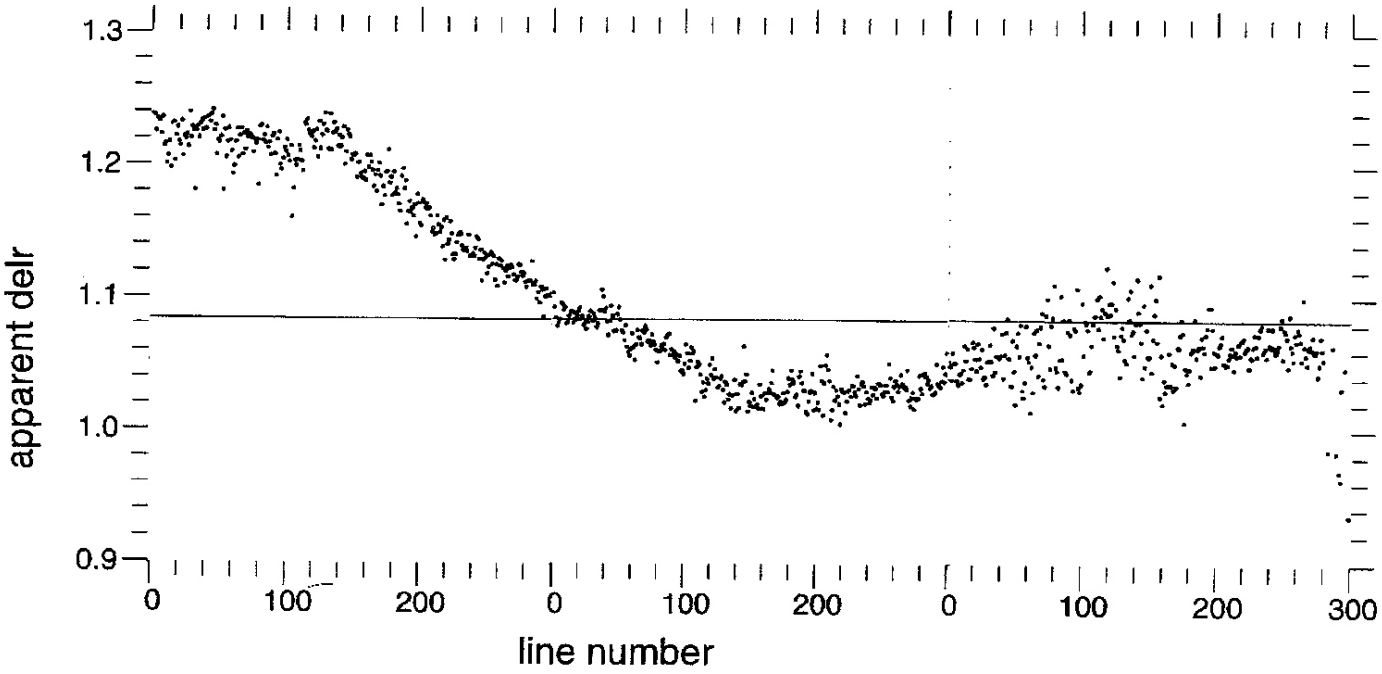

Figure 5. Temporal variation of the apparent range increment over 90 seconds for 900 consecutive raster lines of WSRA wave topography during Hurricane Ike.

elements comprised of 48 microchip patches. The 62 along-track strips are spaced as half wavelength intervals (0.9375 cm) across the width of the antenna (from left to right across the aircraft frame). Each strip produces a narrow beam in the along-track direction and a fan beam in the cross-track direction. Each of the 62 return pulses are dechirped to provide a range profile return for each antenna element and then combined coherently with various phase shifts to produce 80 narrow beams at various angles in the cross-track direction, 13 of which were indicated in Figures 3 and 4. The cross-track spacing of the strips and the phase shifts added to the returns from the 62 individual fan beams before coherently combining them determines the angle that each of the 80 narrow composite beams looks at in the cross-track direction.

The curvature of the mean sea surface in evidence in Figure 4 could also have been caused by the angles of the 80 beams differing from their nominal values. The range to MSL at an angle Θ from height h is

$$r = h / \cos\Theta \approx h + h\,\Theta^2/2.$$

If the actual angle differs from the nominal value by a small fraction d, ie. $\Theta_a = (1+d)\,\Theta$, then

$$r_a \approx h + h\,\Theta_a^2/2 \approx h + h\,\Theta^2/2 + h\,d\,\Theta^2 \approx r + h\,d\,\Theta^2$$

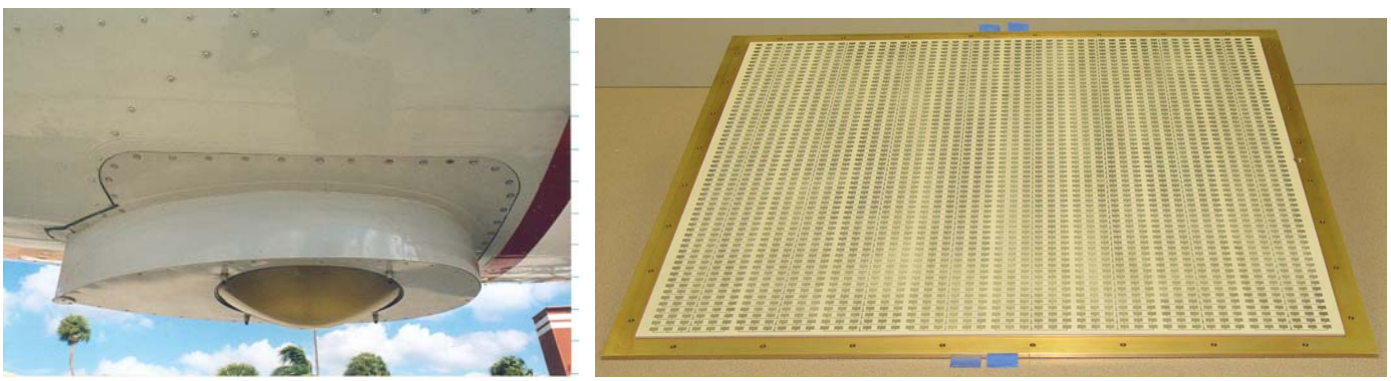

Figure 6. SRA dielectric lens antenna (left) and WSRA microstrip patch antenna (right).

and the apparent range error will increase parabolically with the nominal off-nadir angle. The top panel of Figure 7 shows the effect of the beam angles being 7% larger than their nominal values. When the range data from the larger incidence angles are ascribed to the smaller nominal beam angles, it extends below MSL. In the bottom panel, when range data from smaller incidence angles are attributed to the larger nominal incidence angles they are pulled above MSL.

After the curvature in the mean sea surface was discovered, Ivan PopStefanija doubled checked the software and the various phase shifts added to the 62 fan-beam return waveforms in the raw data processing and found them appropriate for the cross-track spacing of the antenna elements to form the desired 80 composite narrow beams at the nominal angles. The software and the array of phase shifts used to generate the 80 beams did not vary with time so it seemed unlikely, even if they were in error, that they could have been the cause of the temporal variation in evidence in Figure 5. Also, ground tests of the WSRA had confirmed that the detected targets appeared at the expected locations in the generated images when using the nominal values for the cross-track angles.

There were some hardware problems that also lead the investigation astray. There was a phase lock loop to maintain an exact synchronization between the transmitted chirp signal and the chirp signal generated to mix with the returning signal. The loop was noticed to be out of phase lock during the flight into Hurricane Ike. That would have degraded the data, but was unable to explain the abnormal sea surface curvature. In examining the raw return waveforms from the fan beams produced by the 62 linear elements making up the WSRA antenna, it was discovered that the returns from elements 27 and 28 were missing, leading to speculation that a sequencing problem might exist in the 62 transmissions. Testing discovered a faulty switch whose 25 dB insertion loss had simply attenuated the signal of those two elements below the noise floor.

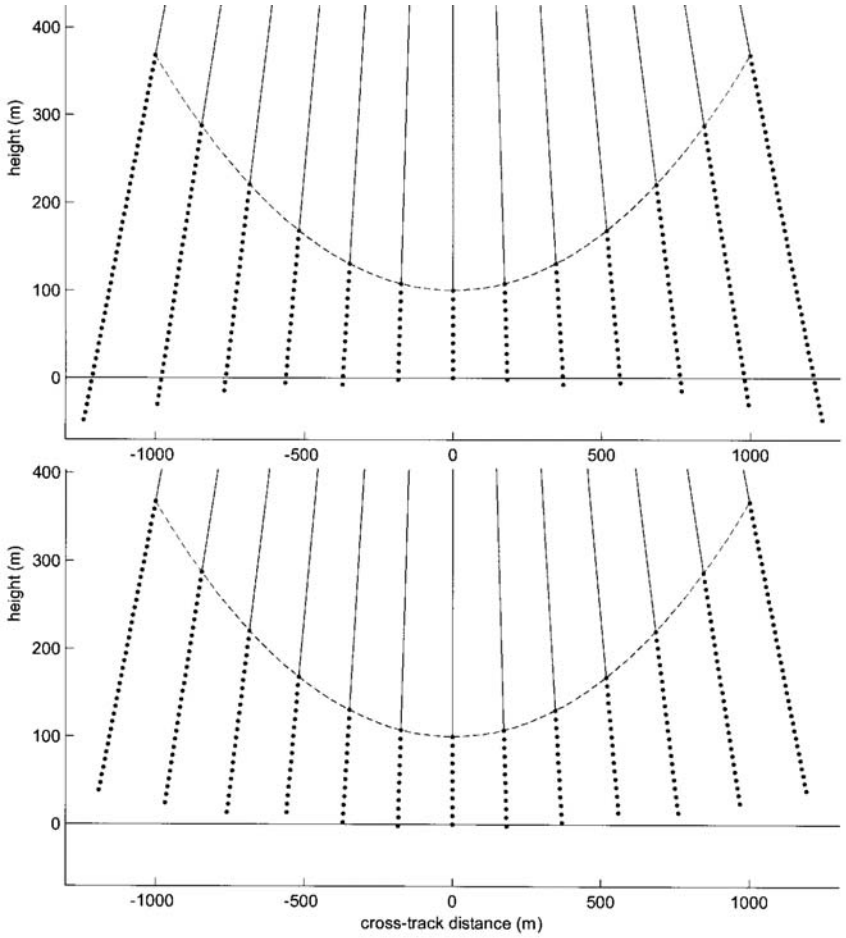

Figure 7. Effect on the apparent range to the sea surface if the separation angles between the beams are 7% larger than the nominal values (top) or 7% smaller than the nominal values (bottom).

ProSensing has fixed the phase lock loop instability and repaired the defective switch. The WSRA system was shipped to AOC on 17 November to be installed on N42RF for flight testing.

The problem in the wave topography was resolved with the best possible outcome. It was not a hardware problem at all! I'll begin my explanation by reviewing the characteristics of the flight into Hurricane Ike.

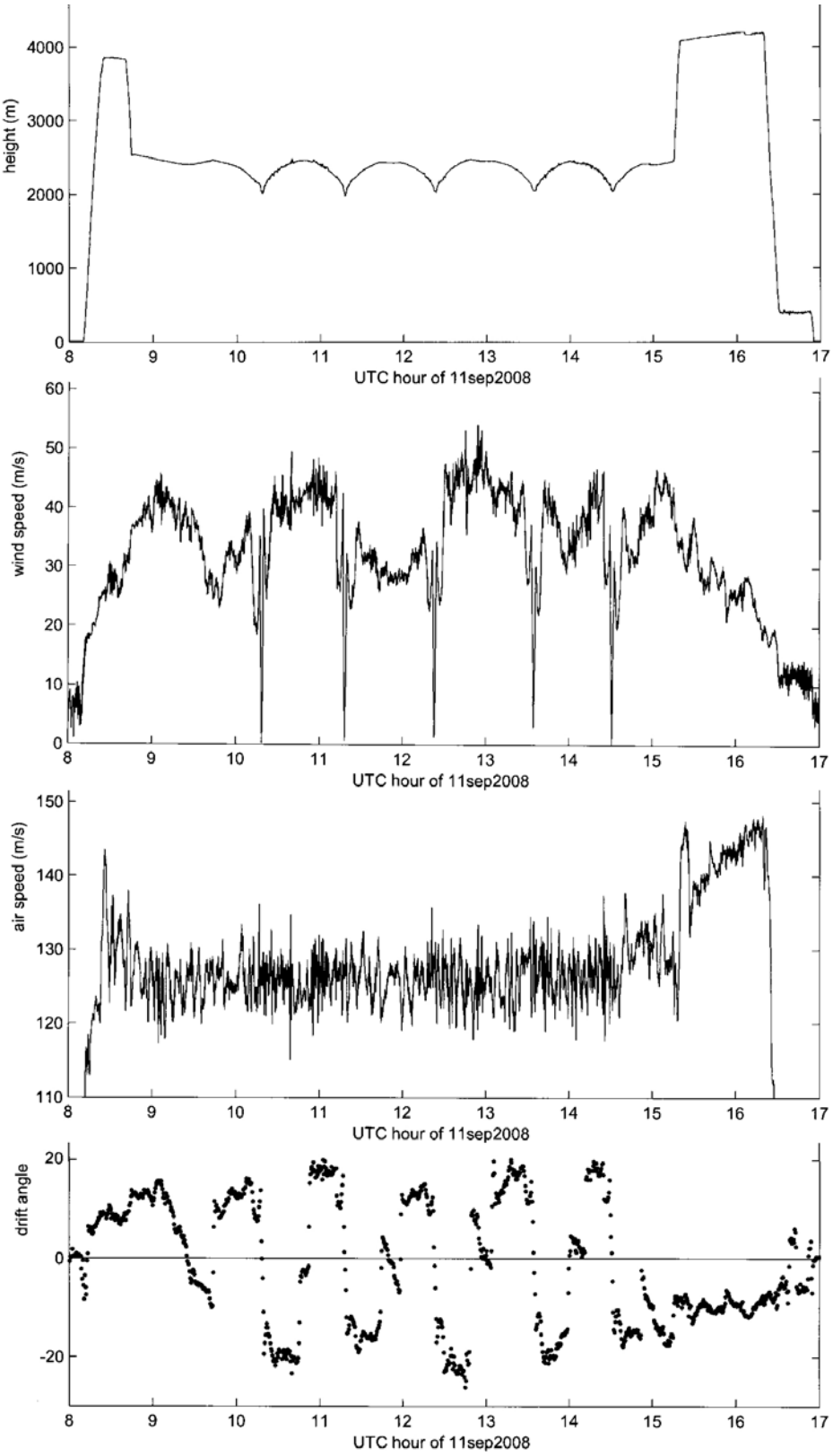

Figure 8. Parameters of the flight of N43RF into Hurricane Ike.

Figure 8 gives an overview of the Hurricane Ike flight on 11 September 2008. The top panel shows the aircraft height variation over a nine hour period. The aircraft took off from MacDill Air Force Base after 0800 and climbed to almost 4 km height for the transit to Ike. It descended to about 2500 m when it arrived in the vicinity of Ike. A little before 1000 it began a series of five eye penetrations. The position of Ike and the plan view of the aircraft track in the vicinity of Ike are shown in Figure 1. During eye penetrations the aircraft autopilot is normally set to maintain a constant barometric altitude which results in the characteristic oscillation in the actual aircraft height because the barometric pressure is significantly lower in the eye. The aircraft then climbed above 4 km for the transit back to MacDill, where it made passes over Tampa Bay at 400 m before landing.

The second panel indicates that the wind speed at the aircraft height in the vicinity of Ike was generally between 30 and 50 m/s except for dropping nearly to zero as the center of the eye was approached. The third panel indicates that the airspeed of the aircraft averaged about 125 m/s during the eye penetrations. The bottom panel indicates that aircraft drift angle (aircraft ground track angle minus aircraft heading), sometimes referred to as the crab angle, oscillated between about 20° and -20° during the eye penetrations.

The aircraft ground track with wind barbs shown in Figure 9 indicates why the drift angle oscillated. As the aircraft approached the eye from any direction, it was subjected to a very strong wind from the left. The aircraft would have to point its nose about 20° to the left so the cross-track component of its airspeed would cancel the cross-track component of the wind speed and allow it to proceed along the desired ground track. As the aircraft departed the eye in any direction, it was subjected to a very strong wind from the right and would have to point its nose about 20° to the right to maintain the desired ground track.

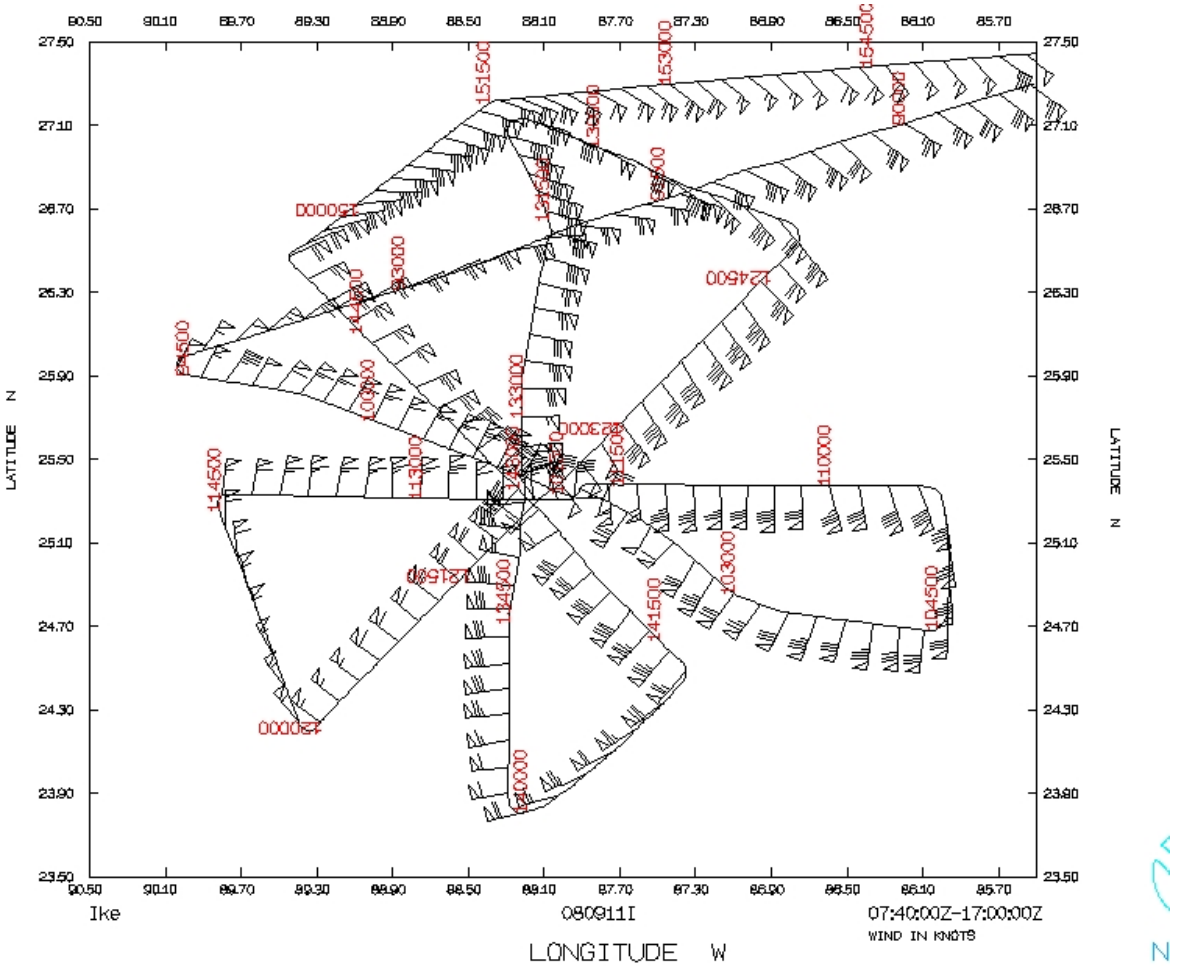

Figure 9. N43RF track in the vicinity of Hurricane Ike with wind barbs.

To compensate for the low peak transmitted power, the WSRA transmits a chirped pulse whose duration is nearly as long as the round trip transit time to the surface. The returning pulse it then mixed with the same chirped signal offset in frequency by the IF to produce the return waveform within the range window. So the transmission and reception process would take a minimum of twice the round trip transit time. At 3 km height that would be 40 μs and permit a pulse repetition frequency (PRF) no higher than 25 KHz.

As the altitude is lowered the transmitted pulse duration shortens and the PRF can be increased. The WSRA PRF would be about 30 KHz at 2 km altitude and 40 KHz at 1.5 km altitude. At 400 m altitude the WSRA PRF would be only 100 KHz because the time required by the supporting hardware functions is a higher fraction of the round trip transit time. Since the WSRA has only one transmitter/receiver which is switched sequentially from element 1 to 2 to 3 … to 62, the process of generating the 62 returns to combine coherently to produce the 80 narrow beams requires 3.1 ms at 3 km height. Suppose element 1 is at the left edge of the antenna, element 62 is at the right edge, and there is a 50 m/s crosswind from the left. Then the antenna would shift gradually to the right by 0.155 m, more than a quarter of its width, during the 62 transmissions. This effective widening of the antenna would change the angles of the 80 composite narrow beams proportionally. Similarly, if the crosswind were from the right, it would effectively narrow the antenna be the same amount and change the 80 beam angles proportionally. This is the process which generated the apparent curvature in the mean sea surface through the effect related to Figure 7.

Even though the WSRA antenna is a rigid, nearly square rectangle, its effective shape in the presence of a strong wind deforms to a parallelogram. For an airspeed of 125 m/s, Figure 10 shows the effective WSRA antenna shapes for four PRFs, three wind speeds and five wind directions relative to the airspeed vector. The effective deformation is largest at the lowest PRF of 20 KHz, corresponding to the highest altitude, and diminishes with increasing PRF (decreasing altitude). The effective modulation of the width widens or narrows the angular spacing of the 80 composite narrow beam.

The shifting in the along-flight direction degrades the beam formation because of decorrelation in the interaction of the scatterers illuminated by the 62 fan beams.

Figure 11 shows that during the radial passes through the eye of Hurricane Ike the wind direction was generally between 45° and 90° from the heading (airspeed direction) of the aircraft. Under those circumstances the effective shape of the antenna would range between the solid and dashed red lines in Figure 10 and the solid and dashed blue lines. After this effect was recognized, ProSensing implemented an operator option to be able to reverse the direction of sequencing through the 62 linear elements of the antenna. So if the wind was from the left, the transmission sequence could move from left to right and if the wind was from the right, the transmission sequence could move from right to left. That would ensure that the effective aperture was generally wider than the physical aperture.

The phase shifts added to the various returns from the 62 transmissions will remain the same, but the cross-antenna component of the wind and the PRF will be used to determine the effective width of the antenna and the actual angles of the 80 composite beams to generate the sea surface topography.

3. WSRA BACKSCATTERED POWER MEASUREMENTS

Figure 12 demonstrates the potential benefits of the WSRA backscattered power measurements. At 1019 UTC the aircraft was leaving the eye of Hurricane Ike and beginning its transit through the eyewall. The top panel shows the SFMR measurements of wind speed and rain rate with the dashed vertical lines identifying eight approximately 10 s intervals during which 100 raster lines of wave topography and backscattered power were acquired by the WSRA.

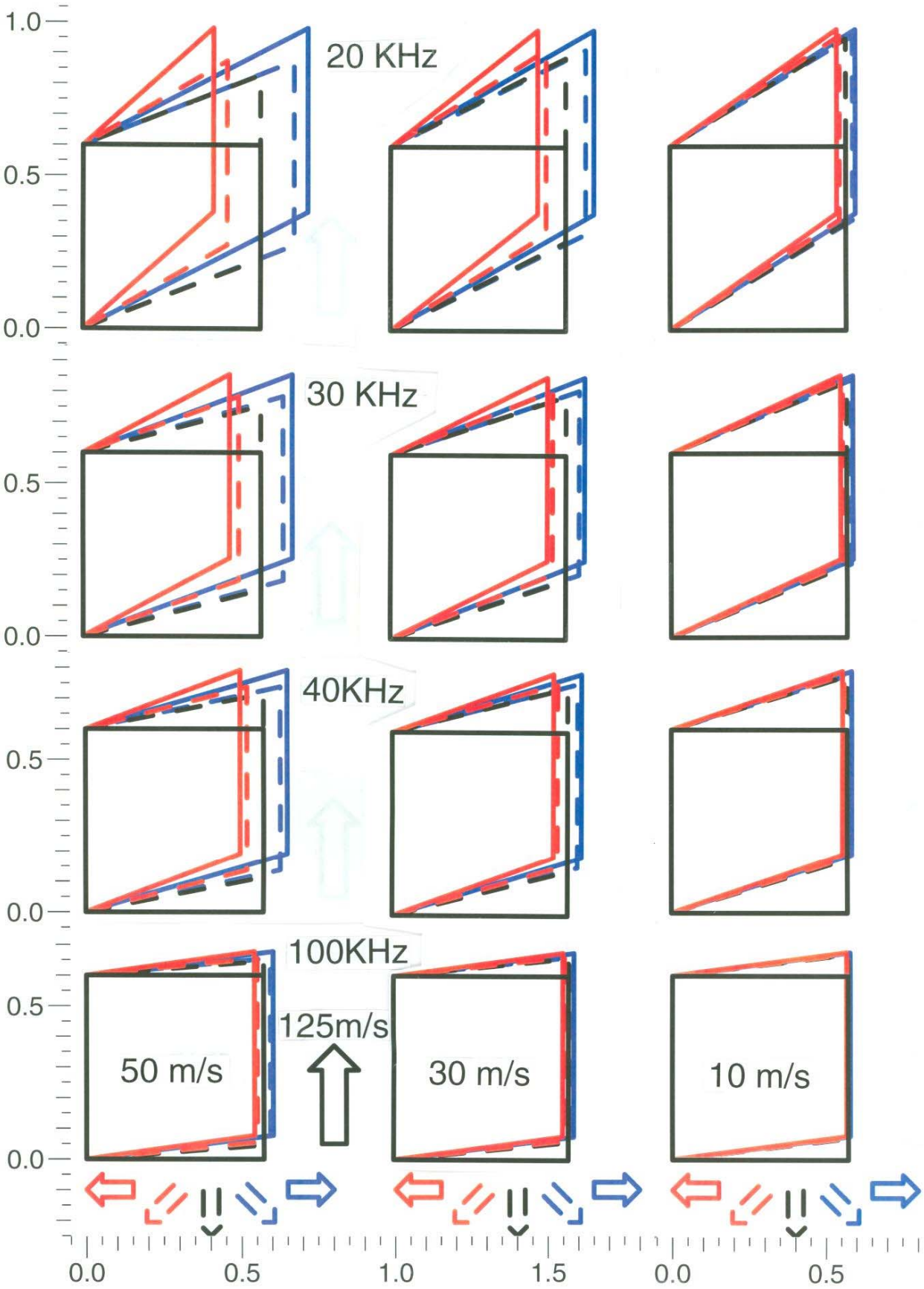

Figure 10. The solid black rectangles in each panel indicate the actual shape of the WSRA antenna, 0.6 m in the direction of flight and 0.57 m across the aircraft. The dashed black and colored parallelograms indicate the effective shapes of the WSRA antenna for an airspeed of 125 m/s in the direction indicated by the black arrow, wind speeds of 50, 30 and 10 m/s blowing in the directions indicated, and transmissions at pulse repetition rates of 100, 40, 30 and 20 KHz, corresponding to aircraft heights of about 0.4, 1.5, 2 and 3 km.

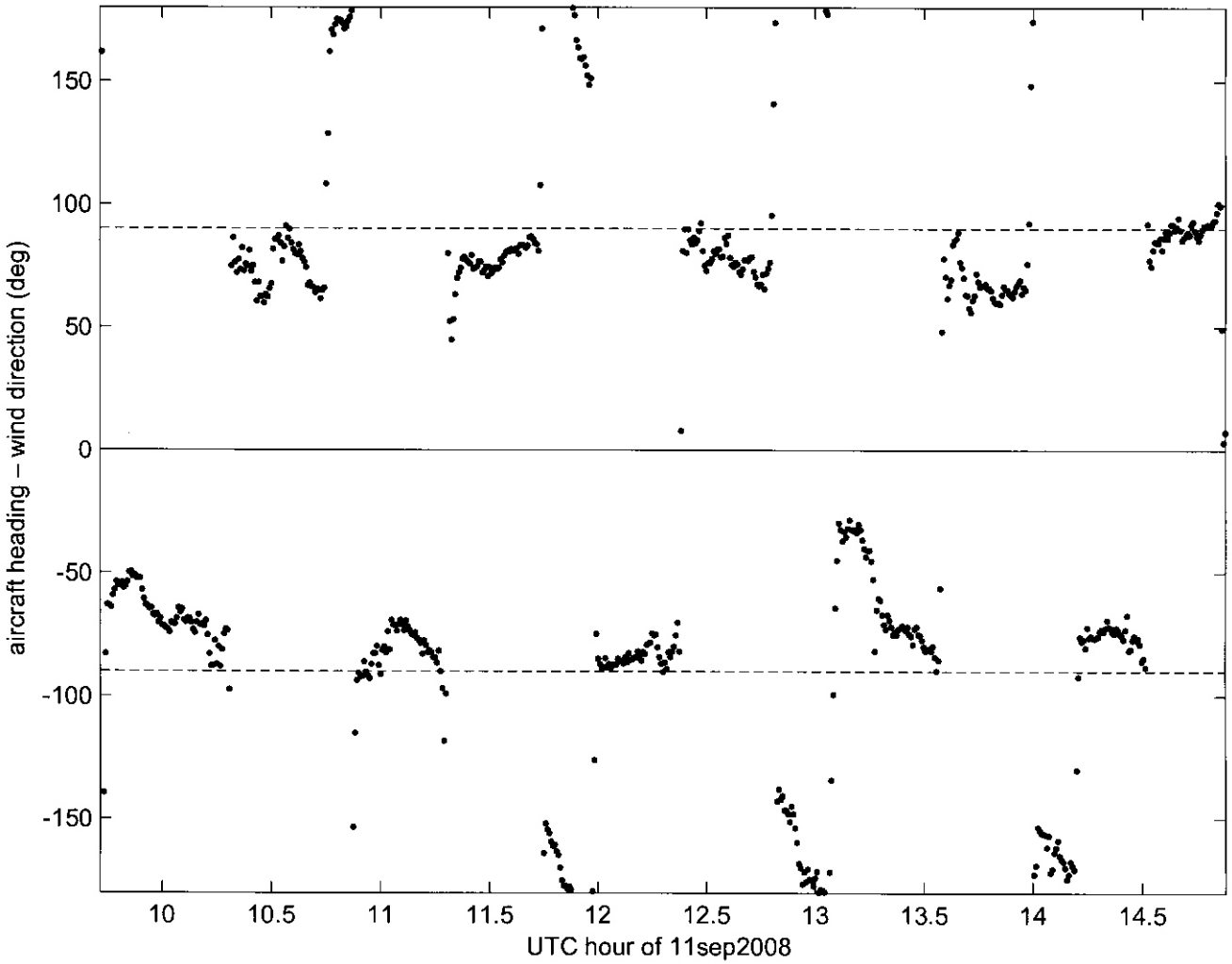

Figure 11. Wind direction relative to aircraft heading (WSRA antenna orientation).

The bottom two panels of Figure 12 show the variation of backscattered power with off-nadir incidence angle for each 100-line average from the eight segments. These data can provide additional information on rain rate and the sea surface mean square slope (mss). To first order, the power backscattered from the sea near nadir is Gaussian distributed in incidence angle with its peak value inversely proportional to mss and its falloff with incidence angle also inversely proportional to mss. When the log of the backscattered power is plotted against the square of the incidence angle tangent, the result is a straight line to first order.

At the WSRA 16 GHz operating frequency, the attenuation coefficient is nearly linearly related to rain rate, being a little less than 1 dB/km for a 15 mm/hr rain rate and a little more than 2 dB/km at 30 mm/hr. The aircraft altitude was a little over 2100 m during the data acquisition shown in Figure 12 and the round trip path loss would have been over 8 dB. The WSRA is 6 times less sensitive to rain attenuation than its SRA predecessor, which operated at 36 GHz, and will rarely cease to function in heavy rain. Curve 8 in the right lower panel of Figure 12 indicates that the WSRA still had at least 13 dB of signal margin even at a rain rate of 30 mm/hr.

Even though the WSRA is less sensitive than its predecessor, it is still 8 times more sensitive than the SFMR, whose frequency is even lower and uses the same absorption technique to determine rain rate. The WSRA may be able to determine light rain rates more accurately than the SFMR because of its higher sensitivity.

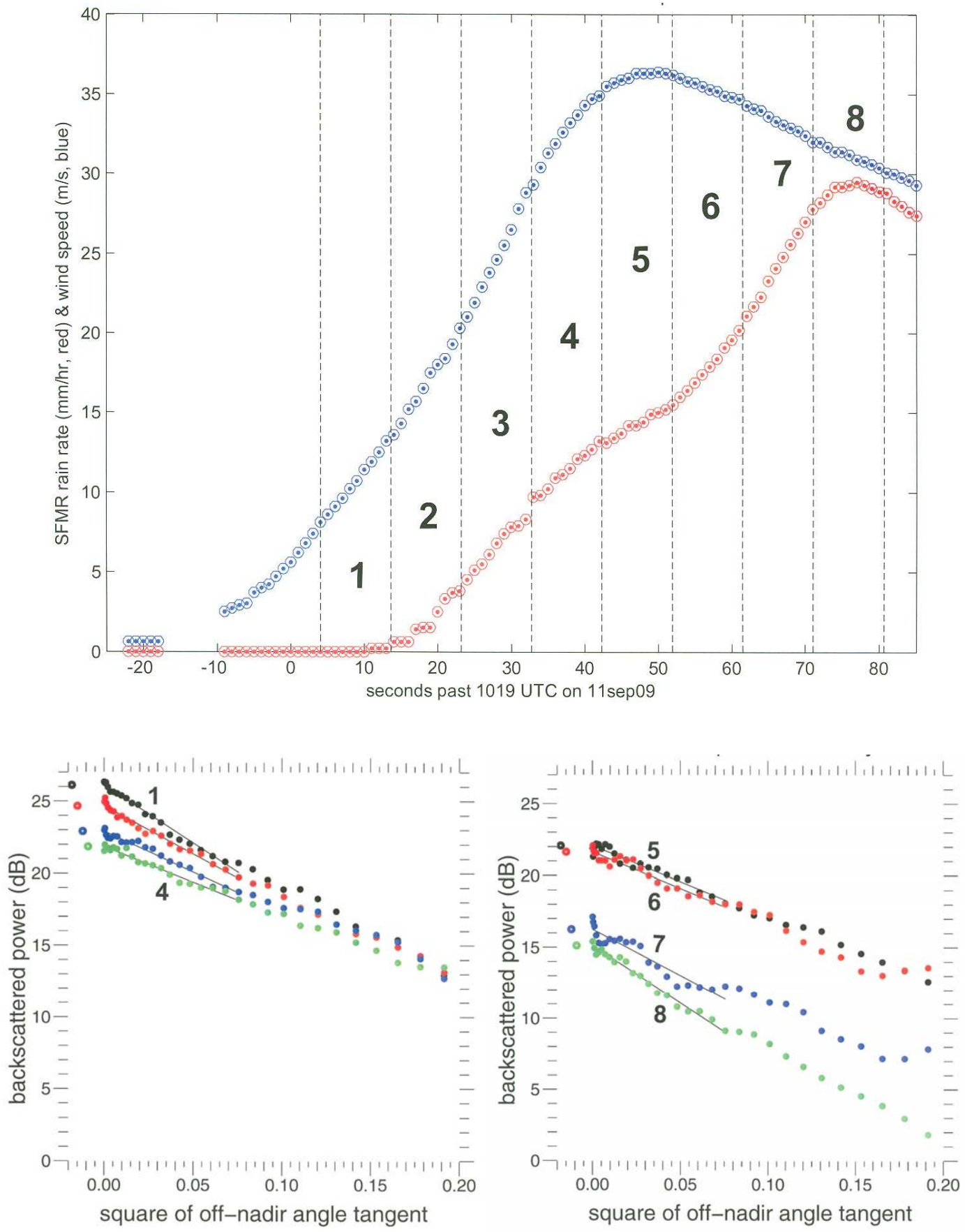

Figure 12. SFMR surface wind speed and rain rate (top panel) and WSRA backscattered power variation (bottom panels). The dots to the left of data indicate the nadir value of the backscattered power determined by the straight lines least squares fitted to data within 15° of nadir.

When the WSRA enters a region of rain, the wind speed and mss will also generally vary, as indicated in Figure 12. The total WSRA signal loss in Figure 12 between region 1 and region 8 was about 11 dB, but less than 9 dB were accounted for by rain attenuation. The remaining loss was due to an increase in mss caused by the higher wind speed in region 8. But it is possible to determine the change in mss from the change in backscatter falloff slope with incidence angle. As the wind speed increases in regions 1 through 4, the slope of the lines fitted to the backscattered power data diminish. This allows for the determination of the mss in any region independent of the rain rate and for the normalization of all the nadir power values to a constant mss. Then any decrease below the maximum value is due solely to rain attenuation.

Higher quality, registered maps of wave topography and backscattered power also offer the possibility of being able to examine surface roughness variations over the dominant waves in a hurricane. It might be possible to investigate whether there is more flow separation (lower mss) on the lee side of waves in the right front quadrant of a hurricane where the wind is blowing perpendicular to the dominant wave crests than in the left front quadrant where the wind is blowing parallel to the dominant wave crests.

4. STATUS OF REAL-TIME DATA TRANSFER AND DISPLAY SOFTWARE

After the raw WSRA data is processed on the aircraft during the flights by the WSRA backend computer, the output data files will be sent via FTP to an aircraft onboard server which will automatically relay them to a ground FTP site (flightsciences.noaa.gov) at AOC and into a dedicated WSRA directory (pub/wsra) that John Hill (AOC) has set up. Jose Salazar (NHC) has already established and configured the WSRA processing and display application on the JHT Muskie server with the aid of a Perl driver which runs the entire application. The process sets up a program to keep checking the public site at AOC for new or updated data files via FTP. Those files are extracted, decompressed and accordingly renamed in order to match the requirements from the WSRA executable. That executable generates the real time WSRA data files to be displayed on NMAP2 within the NAWIPS environment having the necessary map and data tables to access environmental variables as required by the application. With these systems in place and the hardware uncertainties resolved, the WSRA should become operational for the 2010 hurricane season.

5. POTENTIAL FOR WSRA TRAGETED MEASUREMENTS OF STORM SURGE

The latest in many research papers using directional wave spectra from the NASA SRA has just appeared, this one using SRA to assess and improve the performance of the WaveWatch III numerical wave model.

Fan, Y., I. Ginis, T. Hara, C. W. Wright and E. J. Walsh, 2009: Numerical simulations and observations of surface wave fields under an extreme tropical cyclone, *J. Phys. Oceanogr.*, **39**, 2097–2116.

The WSRA is ready to carry on that function. But there is another important potential function for the WSRA that the SRA has only just demonstrated - storm surge measurement.

Wright, C. W., E. J. Walsh, W. B. Krabill, W. A. Shaffer, S. R. Baig, M. Peng, L. J. Pietrafesa, A. W. Garcia, F. D. Marks, Jr., P. G. Black, J. Sonntag, B. D. Beckley, 2009: Measuring Storm Surge with an Airborne Wide-Swath Radar Altimeter, *J. Atmos. Oceanic Technol.*, **26**, 2200-2215.

The WSRA is now the only instrument in the world that could provide targeted storm surge measurements in a landfalling hurricane in the fashion demonstrated by the SRA. That potential WSRA capability was discussed in detail in the mid-year report. Instead of repeating that, what follows in a two-page appendix is the synopsis of the *J. Atmos. Oceanic Technol.* paper that appeared in the October 2009 issue of BAMS. Because of its long lead time, the article erroneously indicated that the WSRA became operational in 2009.

GREEN EGGS AND HAM (AND MILK, AND BREAD, AND . . .)

In Sweden, healthy food isn't just referring to one's body; it's referring to planet Earth. The country is the first to allow food companies to include labels that indicate their foods are climate friendly. Any company that can prove it has reduced greenhouse gas emissions may say so on their products. "The only thing we're guaranteeing is that improvements have been made," says Anna Richert, an advisor to the Federation of Swedish Farmers, who is heading a group that is implementing the new labels. "This could mean reductions in emissions of anything from 5 to 80 percent." A Stockholm milk company that switched from chemicals to manure to fertilize the grass its cows eat is scheduled to be the first to receive the new label. (Source: newscientist.com)

which variable combinations possessed the best classification capacity. Generally, variables that included information about shear or helicity had the greatest classification ability, a result consistent with previous research on the topic.

At 24-h lead times, the probability of detecting a tornado outbreak successfully exceeded 80% when using the optimal variable combinations. The likelihood of falsely detecting the outbreak did not exceed 20%. The skill score, which ranges from 0 (no skill) to 1 (perfect skill) was near 0.7. Values of the statistics degraded with increased lead time, although even at 72 h, 70%–75% of tornado outbreaks were correctly identified by both nonlinear models. Interestingly, logistic regression outperformed support vector machines at longer lead times, whereas for 24-h lead times the two were indistinguishable.

The next phase of this research will consider less distinctive outbreaks and assess additional support vector machine training methods in order to improve on results obtained in this initial study.—Andrew E. Mercer (Cooperative Institute for Mesoscale Meteorological Studies), C. M. Shafer, C. A. Doswell, M. B. Richman, and L. M. Leslie. *"Objective Classification of Tornadic and Nontornadic Severe-Weather Outbreaks," in a forthcoming issue of* Monthly Weather Review.

Measuring Storm Surge with an Airborne Wide-Swath Radar Altimeter

Over the years, hurricane-track forecasts, as well as storm-surge models and the digital terrain and bathymetry data they depend on, have improved significantly. Strides have also been made in knowledge of the detailed variation of the surface wind field driving the surge. The area of least improvement has been in obtaining data on the evolution of the mound of water the hurricane wind and waves push against the shore, which can be used to evaluate the performance of numerical storm surge models. Tide gauges are frequently destroyed by the surge, and surveys done after the event provide no temporal information and only indirect indications of the maximum water level over land. Our research shows that measurements of storm surge using airborne wide-swath radar altimeter technology are sufficiently accurate to help improve the storm surge models.

The landfall of Hurricane Bonnie on 26 August 1998 provided an excellent opportunity to demonstrate the potential benefits of direct airborne measurement of the temporal/spatial evolution of the water level over a large area. Bonnie was a slow-moving storm with a large radius of maximum wind, minimizing both the temporal and spatial gradients. The peak of Bonnie's storm surge was less than 2 m, enabling researchers to demonstrate that even a minimal surge can be well documented. The standard deviation in the NASA Scanning Radar Altimeter (SRA) measurements from their trend

ECHOES

"The way the economy is, nobody is able to just pick up and leave."

—Bryant St. Amant, an oysterman in Bayou La Batre, Alabama, on the recession hindering possible evacuation orders during hurricane season. With people out of work and low on savings, many cannot afford the gas or a hotel stay, which puts more pressure on government agencies to provide aid. Jaime Hernandez, emergency management spokesman for Miami–Dade County, does not believe that the down economy will stop people in the case of an emergency, claiming the county is prepared to shelter about 80,000 residents. (Source: The Associated Press)

was generally less than 10 cm—small compared to differences in Bonnie's surge level between the NOAA operational Sea, Lake, and Overland Surges from Hurricanes (SLOSH) model and the North Carolina State University (NCSU) research model.

The SRA, which was carried by a NOAA hurricane research aircraft through Hurricane Bonnie, demonstrated that an airborne, wide-swath radar altimeter could routinely make targeted measurements of storm surge. In fact, the global positioning system (GPS) aircraft trajectory enabled the instrument to gather survey-quality measurements in-storm, despite a 160-m variation in aircraft altitude, an 11.5-m variation in the elevation of the mean sea surface relative to the ellipsoid over the flight track, and the tidal variation over the 5-h data-acquisition interval.

The NASA SRA was decommissioned after the 2005 hurricane season. The NOAA Small Business Innovation Research (SBIR) program subsequently contracted with ProSensing to build the Wide Swath Radar Altimeter (WSRA) to replace it. The WSRA, with improved data quality and less susceptibility to rain attenuation, became operational in time for the 2009 hurricane season.—C. Wayne Wright (NASA Goddard Space Flight Center), E. J. Walsh, W. B. Krabill, W. A. Shaffer, S. R. Baig, M. Peng, L. J. Pietrafesa, A. W. Garcia, F. D. Marks, Jr., P. G. Black, J. Sonntag, and B. D. Beckley. *"Measuring Storm Surge with an Airborne Wide-Swath Radar Altimeter," in a forthcoming issue of the* Journal of Atmospheric and Oceanic Technology.

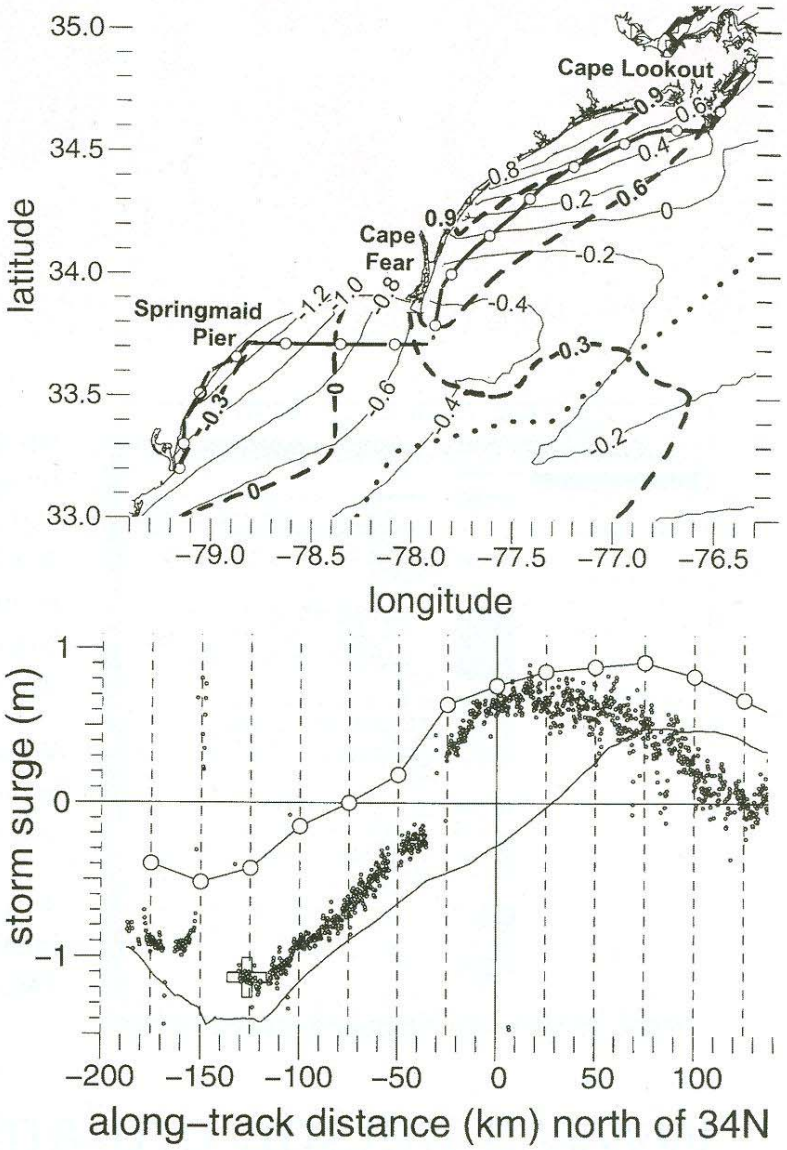

(Top) The aircraft track is superimposed on storm-surge contours from the SLOSH and NCSU models. Circles connected by a thick line identify the aircraft track. Thin lines are NCSU storm-surge model contours, while thick dashed lines indicate SLOSH model contours. Dots mark the western edge of the Gulf Stream. (Bottom) Dots indicate Scanning Radar Altimeter (SRA) storm-surge values along the flight track, with data gaps from land contamination or large aircraft roll attitude. The curve with the circles indicates the SLOSH surge values; the bottom curve is the NCSU surge values along the flight track. The "+" symbol at −126 km indicates the surge value at Springmaid Pier, North Carolina, one of four tide gauges used for an in-flight calibration of the SRA range measurements. To first order, the 1-m difference in the model surges and their bracketing of the SRA measurements was caused by using significantly different hurricane tracks (2-h real-time advisories versus post-storm best track), which bracketed the actual track, indicated by the NOAA aircraft eye fixes. (Walsh et al.)